ABSTRACT

Objective: To investigate the remineralisation of chitosan pre-treated enamel white spot lesions (WSLs) by bioglass in the presence of the pellicle layer.

Methods: 50 artificial enamel white spot lesions were created by acidic gel. Two lesions were used to investigate the formation of the pellicle layer by treating with human whole saliva for 3 minutes. 48 lesions were assigned to 6 experimental groups (n = 8): (1) bioactive glass slurry, (2) bioactive glass containing polyacrylic acid (BG+PAA) slurry, (3) chitosan pre-treated WSLs with BG slurry (CS-BG), (4) chitosan pre-treated WSLs with BG+PAA slurry (CS-BG+PAA), (5) "standard" remineralisation solution (RS) and (6) de-ionised water (negative control, NC). Remineralisation was carried out using a pH-cycling model for 7 days. Before each treatment using remineralising agents, 3-minute pellicle was formed on lesions' surfaces. Mineral content changes, surface and subsurface microhardness and ultrastructure were evaluated by Raman intensity mapping, Knoop microhardness and scanning electron microscopy, respectively. Data were statistically analysed using one-way ANOVA with Tukey's test ($p < 0.05$ is considered as significant).

Results: Despite the heterogeneously formed pellicle layer, all groups showed an increase in surface mineral content after pH-cycling. Chitosan pre-treatment enhanced the subsurface remineralisation of WSLs using bioglass as both pre-treated groups showed greater surface and subsurface microhardness compared to NC. CS-BG exhibited denser subsurface structure than BG, while in CS-BG+PAA the crystals were bigger in size but resemble more enamel-like compared to BG+PAA as shown in SEM observations. Remineralisation of RS was limited to the surface as no significant subsurface changes of mechanical properties and structure were found.

Conclusions: Chitosan pre-treatment can enhance WSL remineralisation with bioglass biomaterials when a short-term salivary pellicle is present. A further investigation using a long-term pH-cycling model with mature pellicle is suggested with regards to clinical application.

Clinical significance: Chitosan pre-treatment has the potential in clinical application to remineralise subsurface lesions to achieve lesion consolidation.

Keywords: dental caries; chitosan; bioglass; salivary pellicle; remineralisation

1. Introduction

The remineralisation of enamel white spot lesion (WSL), the earliest clinical sign of caries manifesting an intact surface zone and a porous subsurface [1], is a complex physico-chemical process because the mineral crystals remained in the lesion are less reactive [2]. Saliva is a biological factor in dental caries which plays numerous roles including neutralizing the acid, providing mineral ions to assist remineralisation and forming the protective acquired enamel pellicle [3,4,5].

The acquired enamel pellicle (AEP) is an organic film forms on enamel surface within minutes after exposure to saliva [6]. This tenacious layer is thought to be insoluble in oral fluids and can grow 0.1 to 1.0 μm in thickness and thus establishes the foundation for the development of dental plaque [5,7]. Many saliva components are found to exist in the pellicle, including proline-rich proteins, statherin and mucinous proteins, and calcium ions chelated by salivary proteins [8,9]. The pellicle has been found to play an important role in reducing enamel demineralisation. Investigations suggest that the pellicle protects enamel against acidic challenge by reducing the dissolution rate of enamel [6]. Featherstone et al. revealed that only aged pellicles formed for 72 and 168 hrs reduced both surface mineral loss and lesion depth compared to untreated [10]. In-situ study found that the pellicle as young as 3 minutes is effective in inhibiting acidic-induced demineralisation by acting as a perm-selective membrane and regulating the diffusion of the acidic agents [11]. This study also concluded that the pellicle layer could also influence the diffusion of calcium and phosphate ions. In addition to these beneficial effects, the pellicle, however, has been found to inhibit crystal growth. In a study into the role of fluoride on apatite growth, crystal will not grow on the site optimally covered by PRP-3 proteins [12], which is also one of major components found in the pellicle both *in vivo* and *in vitro* [13,14]. Such an inhibitory effect is also found to be associated with pellicle statherin peptides, where a covalently linked phosphate group in statherin peptides modulates the inhibition of hydroxyapatite growth [15]. Thus, the pellicle influences the de-/remineralisation balance as a complex biological role.

Many protocols have been developed in an effort to remineralise enamel WSLs, including bioglass [16,17,18,19]. Milly et al. [20] studied enamel WSL remineralisation with 45S5 bioglass modified with polyacrylic acid (PAA) which mimics the functional role of non-collagenous proteins in binding the calcium and phosphate ions to form

nano-precursors. Significant mineral deposition occurred as proved by Raman spectra and SEM images, despite the fact there was not significant reduction of lesion depth. Nevertheless, it appears that remineralisation is limited to the surface where the agent is applied, which is also an issue when using other materials such as fluoride [21]. It is likely that fluoride is more effective in remineralising the surface layer of the carious lesion, leading to surface-blocking which may result in arrested lesion, whereas the remaining porous lesion body becomes less accessible for the remineralising agent and thus will restrict a fuller lesion consolidation [22,23,24]. To overcome this, the delivery of ions into subsurface lesion is pivotal [25]. In this regard, chitosan, an *N*-deacetylated derivative product of chitin, has been incorporated as a potential vehicle to deliver mineral formation ions into deep lesions due to its ability to penetrate enamel [26]. The positive charge of chitosan allows it to adhere to negatively-charged surfaces, including demineralised enamel [27,28]. Recent studies reveal that chitosan-amelogenin (CS-AMEL) hydrogel can induce in-vitro biomimetic remineralisation on enamel lesions, resembling formation of enamel-like crystals and reduction of lesion depth [29]. Remineralisation kept proceeding even when pH decreased below 6.5 due to adhesion provided by the amino groups of chitosan.

However, seldom have investigations taken the pellicle into consideration when evaluating the remineralisation potential of these agents. The fact that the pellicle retards transportation of matter across the enamel may reduce the diffusion rate of ions and thereby affect subsequent remineralisation behaviour [6]. Hence, the aim of this study was to assess the effects of chitosan pre-treatment on in-vitro dynamic remineralisation of artificial WSLs using bioglass biomaterials in the presence of the pellicle layer. Surface mineral content was evaluated by Raman intensity mapping. Surface and cross-sectional microhardness were assessed by Knoop microhardness testing. Scanning electron microscopy was used to study the ultrastructure changes after pH-cycling. The two null hypotheses tested in this study were that the pellicle had no effect on remineralisation and chitosan pre-treatment had no effect on enhancing remineralisation when the pellicle was present.

2. Materials & Methods

2.1 Lesion formation

Fifty caries-free enamel slabs were sectioned off from human molar teeth with ethics approval from NHS Health Research Authority (Reference 16/SW/0220). Slabs were

included in acrylic resin (Oracyl^{TM}, Bracon, UK) in a customised mould for 1 hour with the natural surface facing down. The natural surface was then polished (LabForce-100, Struers, Denmark) with P500 for 10 s, P1200 for 15s, P2000 for 30s and P4000 for 2 min. 1 min and 4 min ultrasonication was carried out between each step and after P4000, respectively, to remove smear layer. Finished surface was protected by nail varnish (Lasting Gel Nail Colour, Collection, UK) to expose a working window about 1 mm wide and 3 mm long.

Demineralisation was conducted using an acidic gel system [20], consisting 8 wt% methylcellulose gel and 0.1 M lactic acid (pH 4.60). The gel was prepared by dissolving methylcellulose powder (Sigma-Aldrich, USA) in boiling deionised water and stirring until room temperature was reached. Maximum five samples were placed on the base of one 250 mL glass beaker and subsequently covered by 100 mL gel, followed by storing in 4^{o}C fridge overnight. Afterwards, a filter paper and lactic acid were sequentially added. The demineralisation was performed in an incubator (MIR-262, Sanyo, Japan) at 37^{o}C for 21 days. Demineralisation solution was refreshed on a weekly basis.

After lesion formation, the acidic gel was removed and rinsed under running deionised water. Nail varnish was removed by acetone, followed by rinsing deionised water.

2.2 In-vitro formation of the pellicle layer

Human whole saliva was collected from one subject. Before collection, the subject was prohibited from eating or drinking. The subject was instructed to chew paraffin gum and saliva was generated, collected in a polystyrene tube (Sterilin^{TM}, Thermo Fisher Scientific, UK) and stored in -80^{o}C freezer. The collected saliva sample had a high buffer capacity (Saliva-Check Buffer Kit, GC, Japan) with a pH of 7.60. The rheological property (spinnbarkeit) was measured to be 2.60 ± 0.32 mm (IMI-0501 NEVA Meter, Ishikawa Ironworks Co., Japan). Before each use, saliva samples were fully defrosted in the tube in a water bath at room temperature.

Two lesion samples were used to investigate the in-vitro formation of the pellicle layer. Saliva was dropped to cover half of the lesion. The culture was conducted for 3 minutes in a mini orbital shaker (SO5, Stuart Scientific, UK) at a shaking speed of 62.5 RPM. Once completed, excessive saliva was gently washed off under running deionised water. Subsequently, lesions were carefully dried using compressed air, and gold-coated for

SEM observations (JCM-6000, JEOL, Japan) in secondary electron mode with acceleration voltage of 15 keV.

2.3 Group assignment

All remaining lesions were assigned to six groups (n = 8): (1) NovaMin^{TM} (BG) slurry, (2) NovaMin^{TM} containing polyacrylic acid (BG+PAA) slurry, (3) chitosan pre-treated WSLs with NovaMin^{TM} slurry (CS-BG), (4) chitosan pre-treated WSLs with NovaMin^{TM}+PAA slurry (CS-BG+PAA), (5) remineralisation solution (RS) and (6) de-ionised water (negative control, NC).

2.4 Baseline surface Raman intensity mapping

Five samples from each group were used for obtaining baseline surface Raman intensity maps. The acquisition was carried out by a micro-Raman spectrometer (inVia Raman Spectroscopy, Renishaw, UK) assembled with a 1200 line/mm grating, using Streamline^{TM} mode at the wavelength of 785 nm. The scanning area was determined by drawing a rectangle on a montage image which included lesion area and untouched sound enamel on both sides. Each area contained 91,000 acquisition points with a step size of 2.7 μm in x and y direction. 960 cm^{-1} was chosen as the monitored peak because it is the strongest peak of phosphate in tooth enamel and can be used to indicate the mineral content [30].

After acquisition, all maps were processed using in-house software. Afterwards, fitted peak height maps were analysed by ImageJ (NIH, US) for the quantification of surface mineral content. The intensity ratio of lesion/sound enamel (I_{lesion}/I_{sound}) at 960 cm^{-1} was calculated to indicate the mineral content of the artificial lesion assuming sound enamel was 100 % in mineral content.

2.5 Baseline surface microhardness

Surface microhardness (SMH) was carried out on the same samples by a microhardness tester fitted with a Knoop diamond indenter (Duramin, Struer, Denmark). A load of 10 gf and dwell time of 5 s were used. For each sample, 5 indentations were measured with a spacing of at least 50 μm.

2.6 pH-cycling regime

In the present study, a pH-cycling model adapted from Karlinsey [31] was incorporated as described in Fig. 1. All chemicals were summarised in Table 1. In general, each cycle

included a three-minute treatment in the morning, an immersion in artificial saliva for two hours, an acidic challenge in the lesion formation gel for four hours, followed by another two-hour immersion in artificial saliva and three-minute treatment, and finally a storage in artificial saliva overnight.

Before the first cycle, sound enamel was protected with acid-resistant tape to minimise contaminants from treatments. Prior to each three-minute treatment, the pellicle layer was formed in the fashion as described in section 2.2. Afterwards, CS-BG and CS-BG+PAA groups were pre-treated with chitosan solution, which was prepared by dissolve 25 mg chitosan (50 to 190 kDa, Sigma-Aldrich, US) in 10 mL acetic acid (0.1 M) and stirred overnight at room temperature to form an aqueous solution of 2.5 mg/mL [26]. After pre-treatment, excessive chitosan was carefully washed off by deionised water.

To prepare BG slurry (1 g/mL), 1 g powder was fully mixed with 1 mL deionised water using a whirlmixer for 1 min. The pH was 12.7. To prepare BG-PAA slurry (1 g/mL, 60/40 wt/wt), 0.6 g BG, 0.4 g PAA powder and 1 mL deionised water were mixed by a whirlmixer for 1 min. The pH was 8.1. The treatment was carried out using a toothbrush machine (Toothbrush, Syndicad, Germany) adapted with microbrush (Benda® Microtwin®, CENTRIX, Australia) at a speed of 1 second per stroke (180 strokes overall). The applied load was approximately 10g. Samples were fixed and remineralising slurries or solutions were applied directly on the lesion surface. After brushing, samples were thoroughly rinsed with deionised water.

After pH-cycling, samples were rinsed with running deionised water to remove any remnants on the lesion surfaces. Protection tape was removed and samples were stored in deionised water at 4 ^{o}C before use.

2.7 Characterisations post-treatment

To quantify the change of surface mineral content post treatment, Raman intensity mapping was repeated on the same samples used in section 2.4 at the same test area. The change of I_{lesion}/I_{sound} was calculated as:

$$\text{Intensity Change} = \left(\frac{I_{lesion}}{I_{sound}}\right)_{post} - \left(\frac{I_{lesion}}{I_{sound}}\right)_{before} .$$

SMH post treatment was carried out again on the same samples in the fashion described in section 2.5. These lesions were further hemi-sectioned and polished following the same procedure described in section 2.1. Rinse under running deionised water for 1 min was performed instead of ultrasonication cleansing. One half was assigned for cross-sectional microhardness using the same indentation protocol. Due to the limitation of lesion size, only 3 indentations were implemented for each sample with spacing approximating to 100 μm.

Remaining three lesions in each group were fractured to generate two cross-section surfaces. These surfaces were coated with gold and observed by SEM as mentioned in section 2.2.

2.8 Statistical analysis

All Raman and microhardness data were statistically analysed using one-way ANOVA with Tukey's test carried out in SPSS 23 for Windows (IBM, USA). Before ANOVA analysis, the normality and homogeneity of all data were checked by Shapiro-Wilk test and Levene test, respectively.

3. Results

3.1 The pellicle layer on lesion surface

The buffer capacity test revealed that the collected saliva sample scored 12 points, indicating a high buffer capacity. The pH and the spinnbarkeit were measured to be 7.60 and 2.60 ± 0.32 mm, respectively. Fig. 2 shows the structure of lesion surface and the pellicle after three-minute culture. Typical porous structure and some cleavage were clearly revealed on the untouched lesion surface (Fig. 2a). In comparison, such kind of features were absent or replaced by some bumps on the surface with saliva treatment, suggesting the existence of a layer of pellicle was successfully formed after 3 minutes.

3.2 Mineral content

The change of intensity ratio was summarised in Fig. 3. All groups showed an increase of intensity, implying mineral regain on lesion surface. Such increase in BG+PAA and CS-BG+PAA, however, is significantly less compared to that in NC ($p < 0.05$). No statistical difference was found between other groups.

3.3 Mechanical properties

Before pH-cycling, the SMH of all groups was around 60 K.H.N and no statistical difference was found between any groups (Fig. 4), indicating the acidic gel system could produce artificial enamel lesions with reproducible mechanical properties. pH-cycling significantly increased the SMH of all groups except RS and NC ($p < 0.05$). CS-BG had the greatest hardness (168.8 ± 22.4, mean ± S.D.), followed by BG (137.0 ± 16.5), CS-BG+PAA (130.9 ± 12.5), and BG+PAA (99.0 ± 12.8). It was noticed that chitosan pre-treated groups all showed greater hardness recovery than those using the same remineralising slurries without pre-treatment. In addition, both groups containing PAA were weaker in mechanical performance than BG-only groups. The mean hardness in RS and NC showed some recovery after pH-cycling (75.1 ± 10.2 and 80.1 ± 14.3, respectively), despite such increase is not statistically different.

Fig. 5 summarises the cross-sectional microhardness of all groups after pH-cycling. It was obvious that all experimental groups except RS showed significantly greater hardness than NC ($p < 0.05$). Though not significant, but both chitosan pre-treated groups showed a larger mean value compared to pre-treatment-free groups.

3.4 Ultrastructural observations

Fig. 6 revealed the ultrastructure of BG and CS-BG at x4000 (a, c) and x10000 magnification (b, d), respectively. Classical prism structure could be recognised in BG (Fig. 6a) with orientated crystals upwards (Fig. 6b). It seems crystals, resembling thin long plate shape, are densely packed on the upper few microns (Fig. 6b) and become loose in deeper lesion. Whilst in CS-BG, the prism structure is not easy to distinguish (Fig. 6c). Crystals were tightly bonded (Fig. 6c) and this bond was present across the entire depth of the cross-section examined. At higher magnification, the morphology was rougher in BG than that in CS-BG.

Dramatically different morphologies were observed in BG+PAA and CS-BG+PAA (Fig. 7). The top surface in BG+PAA was partly reserved after fracture, whereas in CS-BG+PAA the fracture also caused structure alteration, leaving some voids. Nevertheless, both cross-sections were covered by a layer of coating thus prism could be hardly seen (red arrows, Fig. 7a and 7c). The coating layers were composed of randomly distributed needle-like crystals. It seems the size of crystal in BG+PAA is

smaller both in width and length than that in CS-BG+PAA as revealed in Fig. 7b and 7d.

In terms of RS and NC, prismatic structure was clearly distinguished (Fig. 8). Some parts of prisms in RS were lost (Fig. 8a), which was caused by the fracture. Demineralisation-induced gaps appeared in NC (Fig. 8c). No indication of any kind of newly-grown apatite crystals was seen in both groups. At higher magnification, it was clear that both groups illustrated orientated crystals and gaps, indicating a loosely-bonded structure. Significant mineral deposition occurred as proved by Raman spectra and SEM images, despite the fact there was not significant reduction of lesion depth.

4. Discussion

In the present study, a layer formed after 3-minute culture by human saliva *in vitro* which covered the entire area observed, leading to a sealing of all discernible open pores that can be seen on untreated surface. This is in line with other reports [4,33], suggesting the pellicle layer successfully formed on lesion surface under our experiment conditions. Some heterogeneous agglomerations were also noticed, which is the result of selective adsorption property of pellicle proteins [6].

Although surface voids were blocked by the pellicles, this film seemed not prevent surface remineralisation from taking place because all groups showed an increase of Raman intensity after 7d de-/remineralisation cycling. The increase in RS and NC was majorly attributed to the remineralisation of artificial saliva. However, the mean value of BG, CS-BG, RS and NC is almost the same, implying that the pellicle layer affected the surface remineralisation. It is surprising to see that BG+PAA and CS-BG+PAA groups showed significantly lower mineral regain on the lesion surface compared to NC. This seems to contradict Milly et al.'s findings in which BG+PAA presented similar surface remineralisation potential to BG [20]. It should be mentioned that they did not compare the Raman intensity change before and post treatment but only tested surface after treatment. In addition, their treatment was conducted in the fashion that no mechanical agitation, which implies that BG+PAA had sufficient to remineralise. Unlike other BG-only groups in which slurries were flowable, the poor flowability of the viscos BG+PAA slurries after preparation might inhibit the diffusion of mineral formation and thus slowed down the remineralisation process. This impact is further reflected in the surface microhardness that BG+PAA groups had less hardness recovery.

Chitosan products have been reported to potentiate the remineralisation of artificial white spot lesions *in vitro* as an agent-carrier [29]. There are two possible pathways through which chitosan influences remineralisation, *i.e.* by penetrating into enamel [26] and binding onto demineralised crystals through electrostatic force, or by etching lesion surface due to its acidic pH (3.30). However, it is well understood that the pellicle layer provides a protective effect of enamel from acid challenge due to the adsorption of phosphoproteins and mucins that reduce the solubility of the enamel surface [6]. Hannig et al. [11] proved that 3-minute old pellicle is effective in inhibiting enamel demineralisation. Hence, we speculate that the former pathway is the dominant mechanism. It can be seen from the microhardness results that chitosan-treated groups had a non-significant greater tendency than the other groups not only on the surface but also on the subsurface, which might be caused by the short pH-cycling regime.

Treating lesions with bioglass significantly altered the subsurface structure. Bioglass degrades and releases calcium and phosphate ions and thus functions as external ion source and accelerates remineralisation [19]. Calcium ions are stabilised by chitosan through chelation [34]. As a result, a native enamel-chitosan-calcium structure could form on the subsurface. In our work, crystals in CS-BG were tightly bonded across the entire area observed whereas in BG the prismatic structure was still recognisable and had a rougher appearance. As mentioned above, chitosan could diffuse into lesion subsurface and bind to negatively charged surfaces. Here, it is reasonable to infer that subsurface remineralisation in CS-BG was induced by chitosan which attracted apatite formation ions into deep lesion. Apatite grew on the demineralised surfaces and eventually filled the gaps, leading to a relatively intact subsurface as shown in Fig. 6c. The intact subsurface might be the main reason for the greater subsurface hardness found in CS-BG. Another advantage of chitosan is such kind of polysaccharide can inhibit spontaneous precipitation [34,35]. This can favour a long-term, more complete subsurface remineralisation as fast precipitation can block pathways and reduce the diffusion of remineralising agents [25].

Interestingly, BG+PAA groups showed a significantly different appearance (Fig. 7). In both groups, subsurface was covered by a layer of coating composed of randomly-distributed crystals. Polyacrylic acid has been reported to bind calcium and phosphate ions to induce formation of nano-precursors include amorphous calcium phosphate (ACP) which are small enough to penetrate the lesions [36,37]. Zhang et al. [34] found

that chitosan derivative could promote transformation of amorphous calcium phosphate to enamel-like crystals. Therefore, crystals found in CS-BG+PAA were enamel-like due to the intervention from chitosan, whereas in BG+PAA, the absence of chitosan led to smaller crystals. Nevertheless, it is worth mentioning that the newly-precipitated apatite coating still preserves porosities and even failed to cover the entire subsurface as seen in Fig. 6c. This porous structure might be the major reason that BG+PAA groups had weaker mechanical performance.

The remineralisation ability of "standard" remineralisation solution was limited when a pellicle layer was present, as no statistical difference was found compared to negative control. Both groups also did not show any mineral depositions on the subsurface which remained porous. The pellicle also retards transportation of matter across the enamel surface [38] and inhibits the growth of hydroxyapatite [15]. Even though the pellicle layer could be removed by brushing, the fact that the pellicle, like chitosan, can penetrate enamel in a filamentous manner [6] might still negatively influence the remineralisation. These features might account for the weak remineralisation of RS in the present study. However, this doesn't explain why subsurface remineralisation wasn't inhibited by the pellicles in BG and BG+PAA groups. There is a paucity of investigations incorporating the pellicle in remineralisation of enamel carious lesions using Bioglass and the mechanism underlying remains unknown, but we speculate that BG and BG+PAA created a suitable environment, such as alkaline pH (for BG, the pH instantly increased to 12 after preparation) and high ionic concentration [39], that suppressed the inhibition effect of the pellicles.

The design of this study was to try to evaluate the remineralisation of enamel WSLs pre-treated with chitosan using a more clinically relevant biological model. With this regard, the in-vitro pellicle was formed on artificial lesions before pH-cycling. However, due to the time restriction of each cycle, we wouldn't be able to have matured pellicle, implying that the thickness might be limited. In addition, the pH-cycling only lasted for 7 days. A long-term study with mature pellicle is required to understand the mechanism of pellicle's role in influencing the remineralisation.

5. Conclusions

The two null hypotheses were rejected. The in-vitro pellicle formed after 3-minute culture by human saliva reduced the diffusion rate of calcium and phosphate ions into

subsurface lesion when remineralising with “standard” remineralisation, which showed obvious surface mineral gain but no precipitation on the subsurface. The presence of the pellicle, however, did not affect chitosan’s ability to enhance subsurface remineralisation. CS-BG showed greater surface biomechanical properties and dense subsurface compared to all other groups. Further studies incorporating mature pellicle and long-term pH-cycling regimes are suggested in clinical regards.

Conflict of interest

The authors declare no conflicts of interest with respect to the authorship and/or publication exist in this paper.

References

[1] E.A.M. Kidd, Essential of dental caries: the disease and its management, third ed., Oxford University Press, Oxford, 2005.

[2] J.M. ten Cate, In vitro studies on the effects of fluoride on de- and remineralization, J. Dent. Res. 69 (Spec) (1990) 614-619.

[3] J.D.B. Featherstone, Prevention and reversal of dental caries: role of low level fluoride, Community Dent. Oral Epidemiol. 27 (1) (1999) 31-40.

[4] M. Hannig, M. Balz, Influence of in vivo formed salivary pellicle on enamel erosion, Caries Res. 33 (1999) 372-379.

[5] J. Hicks, F. Garcia-Godoy, C. Flaitz, Biological factors in dental caries: role of saliva and dental plaque in the dynamic process of demineralization and remineralization (part 1), J. Clin. Pediatr. Dent. 28 (1) (2003) 47-52.

[6] U. Lendenmann, J. Grogan, F. Oppenheim, Saliva and dental pellicle - A review, Adv. Dent. Res. 14 (2000) 22-28.

[7] P.D. Marsh, Microbiologic aspects of dental plaque and dental caries, Dent. Clin. North Am. 43 (4) (1999) 599-614.

[8] M. Larsen, E. Pearce, Saturation of human saliva with respect to calcium salts, Arch. Oral Biol. 48 (4) (2003) 317-322.

[9] A. Lussi, A. Bossen, C. Höschele, B. Beyeler, B. Megert, C. Meier, E. Rakhmatullina, Effects of enamel abrasion, salivary pellicle, and measurement angle on the optical assessment of dental erosion, J. Biomed. Opt. 17 (9) (2012) 97009-1.

[10] J.D.B. Featherstone, J.M. Behrman, J.E. Bell, Effect of whole saliva components on enamel demineralization in vitro, Crit. Rev. Oral Biol. Med. 4 (3-4) (1993): 357-362.

[11] M. Hannig, M. Fiebiger, M. Güntzer, A. Döbert, R. Zimehl, Y. Nekrashevych, Protective effect of the in situ formed short-term salivary pellicle, Arch. Oral Biol. 49 (11) (2004) 903-910.

[12] H.C. Margolis, K. Varughese, E.C. Moreno, Effect of fluoride on crystal growth of calcium apatites in the presence of a salivary inhibitor, Calcif. Tissue Int. 34 (Suppl 2) (1982) S33-40.

[13] E.E. Kousvelari, R.S. Baratz, B. Burke, F.G. Oppenheim, Immunochemical identification and determination of proline-rich proteins in salivary secretions, enamel pellicle, and glandular tissue specimens, J. Dent. Res. 59 (8) (1980) 1430-1438.

[14] M.S. Ruan, C. Di Paola, I.D. Mandel, Quantitative immunochemistry of salivary proteins adsorbed in vitro to enamel and cementum from caries-resistant and caries-susceptible human adults, Arch. Oral Biol. 31 (9) (1986) 597-601.

[15] Y. Xiao, M. Karttunen, J. Jalkanen, M.C. Mussi, Y. Liao, B. Grohe, F. Lagugné-Labarthet, W.L. Siqueira, Hydroxyapatite Growth Inhibition Effect of Pellicle Statherin Peptides, J. Dent. Res. 94 (8) (2015) 1106-1112.

[16] A.K. Burwell, L.J. Litkowski, D.C. Greenspan, Calcium Sodium Phosphosilicate (NovaMin®): Remineralisation potential, Adv. Dent. Res. 21 (1) (2009) 35-39.

[17] E.S. Gjorgievska, J.W. Nicholson, I.J. Slipper, M.M. Marija, Remineralisation of demineralised enamel by toothpastes: A scanning electron microscopy, energy dispersive X-ray analysis and three-dimensional stereo-micrographic study, Microsc. Microanal. 19 (3) (2013) 587-595.

[18] A.S. Bakry, H. Takahashi, M. Otsuki, J. Tagami, Evaluation of new treatment for incipient enamel demineralisation using 45S5 bioglass, Dent. Mater. 30 (3) (2014) 314-320.

[19] H. Milly, F. Festy, M. Andiappan, T.F. Watson, I. Thompson, A. Banerjee, Surface pre-conditioning with bioactive glass air-abrasion can enhance enamel white spot lesion remineralization, Dent. Mater. 31 (5) (2015) 522-533.

[20] H. Milly, F. Festy, T.F. Watson, I. Thompson, A. Banerjee, Enamel white spot lesions can remineralise using bio-active glass and polyacrylic acid-modified bio-active glass powders, J. Dent. 42 (2) (2014) 158-166.

[21] C. Robinson, R.C. Shore, S.J. Brookes, S. Strafford, S.R. Wood, J. Kirkham, The chemistry of enamel caries, Crit. Rev. Oral Biol. Med. 11 (4) (2000) 481-495.

[22] J.M. ten Cate, J. Arends, Remineralization of artificial enamel lesions in vitro: III. A study of the deposition mechanism, Caries Res. 14 (6) (1980) 351-358.

[23] N.J. Cochrane, D.T. Zero, E.C. Reynolds, Remineralization models, Adv. Dent. Res. 24 (2) (2012) 129-132.

[24] R.J.M. Lynch, S.R. Smith, Remineralization agents – new and effective or just marketing hype?, Adv. Dent. Res. 24 (2) (2012) 62-67.

[25] B.T. Amaechi, Remineralization therapies for initial caries lesions, Curr. Oral Health Rep. 2 (2) (2015) 95-101.

[26] T.M. Arnaud, B. de Barros Neto, F.B. Diniz, Chitosan on dental enamel de-remineralization: an in vitro evaluation, J. Dent. 38 (11) (2010) 848-852.

[27] P.M. Claesson, B.W. Ninham, pH-dependent interactions between adsorbed chitosan layers, Langmuir. 8 (5) (1992) 1406-1412.

[28] A. Young, G. Smistad, J. Karlsen, G. Rolla, M. Rykke, Zeta potentials of human enamel and hydroxyapatite as measured by the Coulter DELSA 440, Adv. Dent. Res. 11 (4) (1997) 560-565.

[29] Q. Ruan, D. Liberman, R. Bapat, K.B. Chandrababu, J.H. Phark, J. Moradian-Oldak, Efficacy of amelogenin-chitosan hydrogel in biomimetic repair of human enamel in pH-cycling systems, J. Biomed. Eng. Inform. 2 (1) (2016) 119-128.

[30] I. Rehman, L.L. Hench, W. Bonefield, R. Smith, Analysis of surface layers on bioactive glasses, Biomaterials. 15 (10) (1994) 865-870.

[31] R.L. Karlinsey, A.C. Mackey, E.R. Walker, B.T. Amaechi, R. Karthikeyan, K. Najibfard, A.M. Pfarrer, Remineralization potential of 5,000 ppm fluoride dentifrices evaluated in a pH cycling model, J. Dent. Oral Hyg. 2 (1) (2010) 1-6.

[32] J.M. ten Cate, R.A. Exterkate, M.J. Buijs, The relative efficacy of fluoride toothpastes assessed with pH cycling, Caries Res. 40 (2) (2006) 136-141.

[33] K.K. Skjørland, M. Rykke, T. Sønju, Rate of pellicle formation in vivo, Acta. Odontol. Scand. 53 (6) (1995) 358-362.

[34] X. Zhang, Y. Li, X. Sun, A. Kishen, X. Deng, X. Yang, H. Wang, C. Cong, Y. Wang, M. Wu, Biomimetic remineralization of demineralized enamel with nano-complexes of phosphorylated chitosan and amorphous calcium phosphate, J. Mater. Sci. Mater. Med. 25 (12) (2014) 2619-2628.

[35] C.A. wan Andrew, E. Khor, G.W. Hastings, The influence of anionic chitin derivatives on calcium phosphate crystallization, Biomaterials. 19 (14) (1998) 1309-1316.

[36] M. Kamitakahara, M. Kawashita, T. Kokubo, T. Nakamura, Effect of polyacrylic acid on the apatite formation of a bioactive ceramic in a simulated body fluid: fundamental examination of the possibility of obtaining bioactive glass-ionomer cements for orthopaedic use, Biomaterials. 22 (23) (2001) 3191-3196.

[37] F.T. Tay, D.H. Pashley, Guided tissue remineralisation of partially demineralised human dentine, Biomaterials. 29 (8) (2008) 1127-1137.

[38] E.C. Moreno, R.T. Zahradnik, Demineralization and remineralization of dental enamel, J. Dent. Res. 58 (Spec Issue B) (1979) 896-903.

[39] L.L. Hench, The story of bioglass, J. Mater. Sci. Mater. Med. 17 (11) (2006) 967-978.

Table 1 Composition and concentration of applied materials

Material	Compositions
BG slurry (1 g/L)	NovaMin™ 4516 bioactive glass [a] (1 g), deionised water (1 mL)
BG+PAA slurry (1 g/L)	NovaMin™ 4516 bioactive glass [a] (0.6 g), polyacrylic acid powder (0.4 g), deionised water (1 mL)
Chitosan solution (2.5 mg/mL)	Chitosan powder (25 mg), 0.1 M acetic acid solution (10 mL)
"Standard" remineralisation solution [32]	HEPES (20 mM), KCl (130 mM), $CaCl_2$ (1.5 mM), KH_2PO_4 (0.9 mM), pH adjusted to 7.0 by 1 M NaOH
Artificial saliva	$CaCl_2$ (0.7 mM), $MgCl_2$ (0.2 mM), KH2PO4 (4.0 mM), HEPES (20 mM), KCl (30.0 mM), pH adjusted to 7.0 by 1M NaOH

[a] GlaxoSmithKline Healthcare (Weybridge, UK)

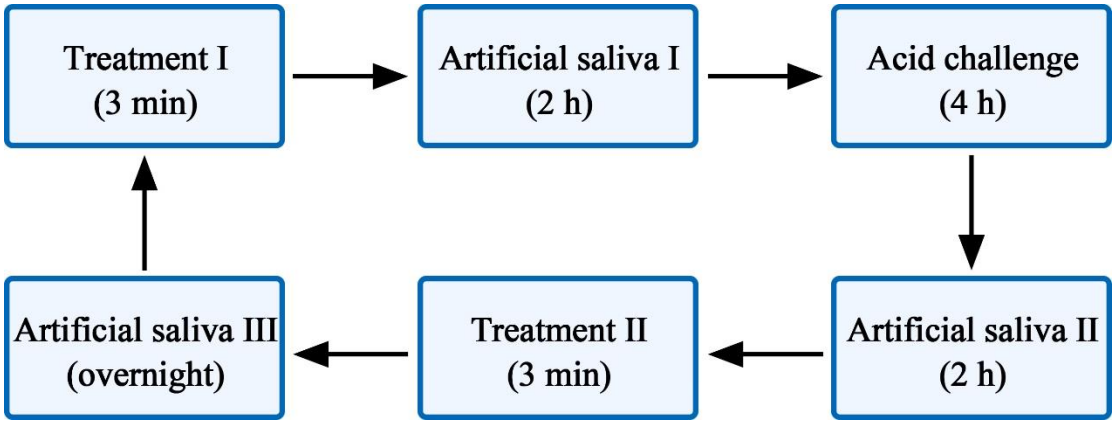

Fig. 1 Illustration of pH-cycling. The entire regime lasted for 7 days.

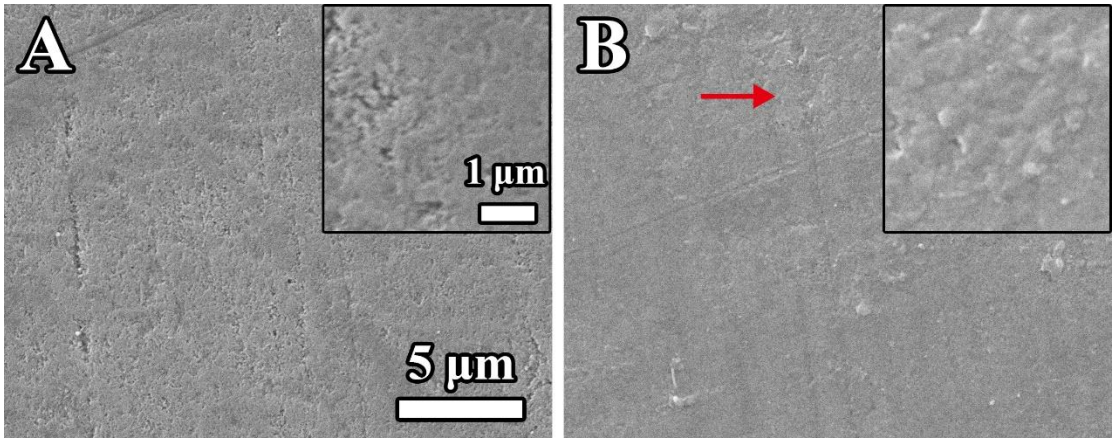

Fig. 2 SEM micrographs (x4000) of lesion surface without (a) and with (b) 3-minute saliva treatment. Untreated lesions surface shows numerous porosities derived from demineralisation. Such kind of pores were sealed, and the surface was covered, indicating the formation of the pellicle layer. Red arrow indicates some agglomerates which might be due to the selective adsorption of pellicle proteins. Insets are observations at higher magnification (x10000).

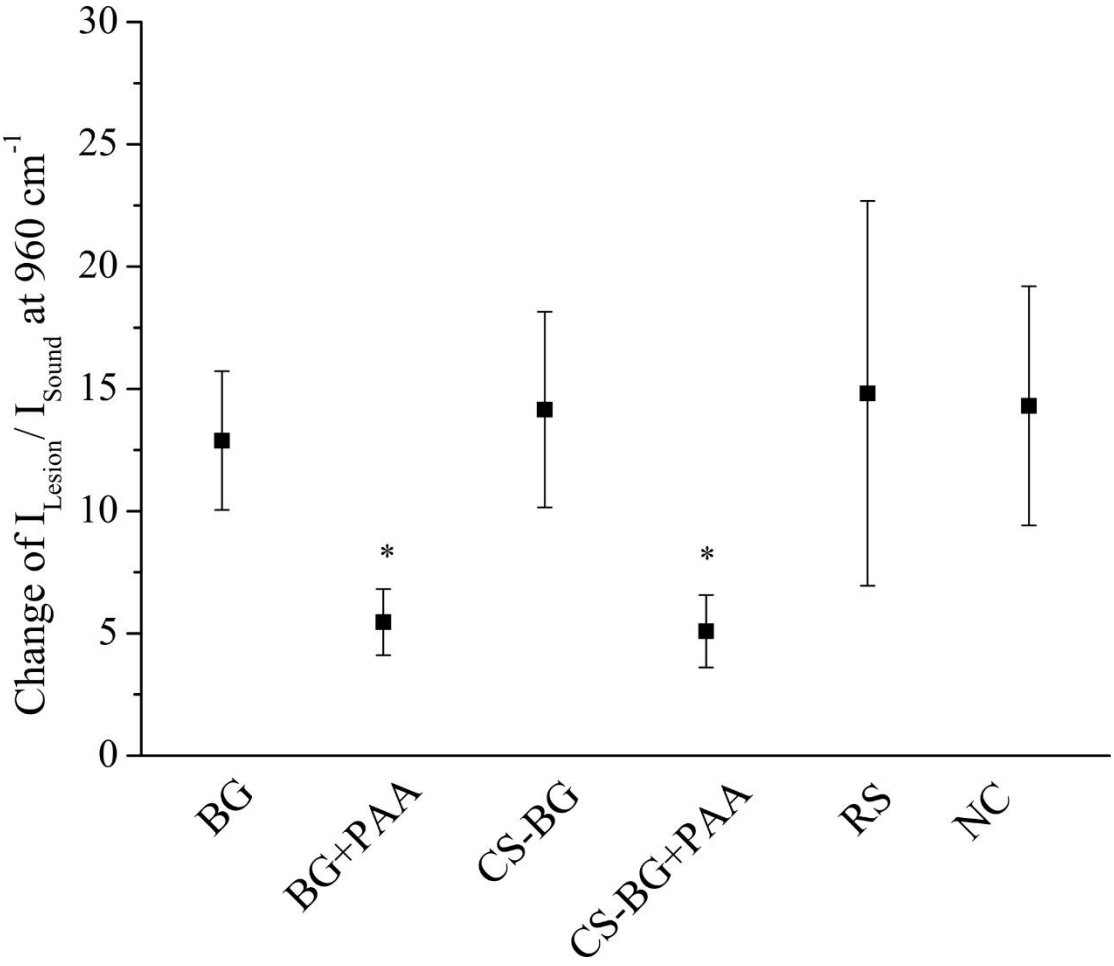

Fig. 3 The change of intensity ratios (I_{lesion}/I_{sound}) of lesion surface at 960 cm^{-1} after 7d pH-cycling. All groups show an increase after treatment, suggesting mineral deposition occurred on the surface. RS and NC have similar mineral regain but with larger standard deviation. Both BG-PAA groups are significantly smaller in mineral regain compared to BG-only groups ($p < 0.05$), which might be due to its viscous status after preparation that retarded the ion movement. "*" indicates statistical difference compared to NC.

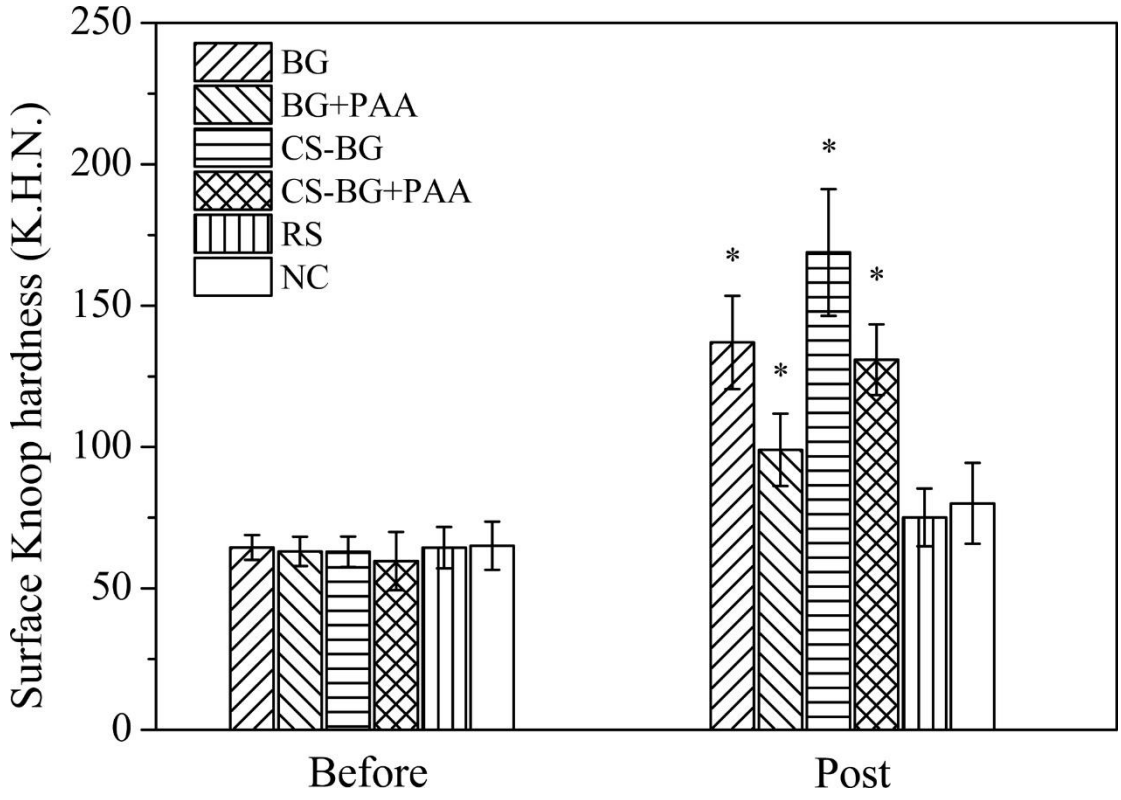

Fig. 4 Surface Knoop microhardness before and post pH-cycling (Mean ± S.D, K.H.N.). All groups have similar microhardness around 60. CS-BG exhibits greatest hardness post treatment, reaching (168.8 ± 22.4), followed by BG (137.0 ± 16.5), CS-BG+PAA (130.9 ± 12.5), and BG+PAA (99.0 ± 12.8), which are significantly greater compared to baseline ($p < 0.05$). In addition, chitosan pre-treated groups show greater mean hardness than those in untreated despite it is not statistically significant ($p > 0.05$). RS (75.1 ± 10.2) and NC (80.1 ± 14.3) exhibit some increases but not significant. "*" indicates statistical difference compared to the value before treatment in the same group.

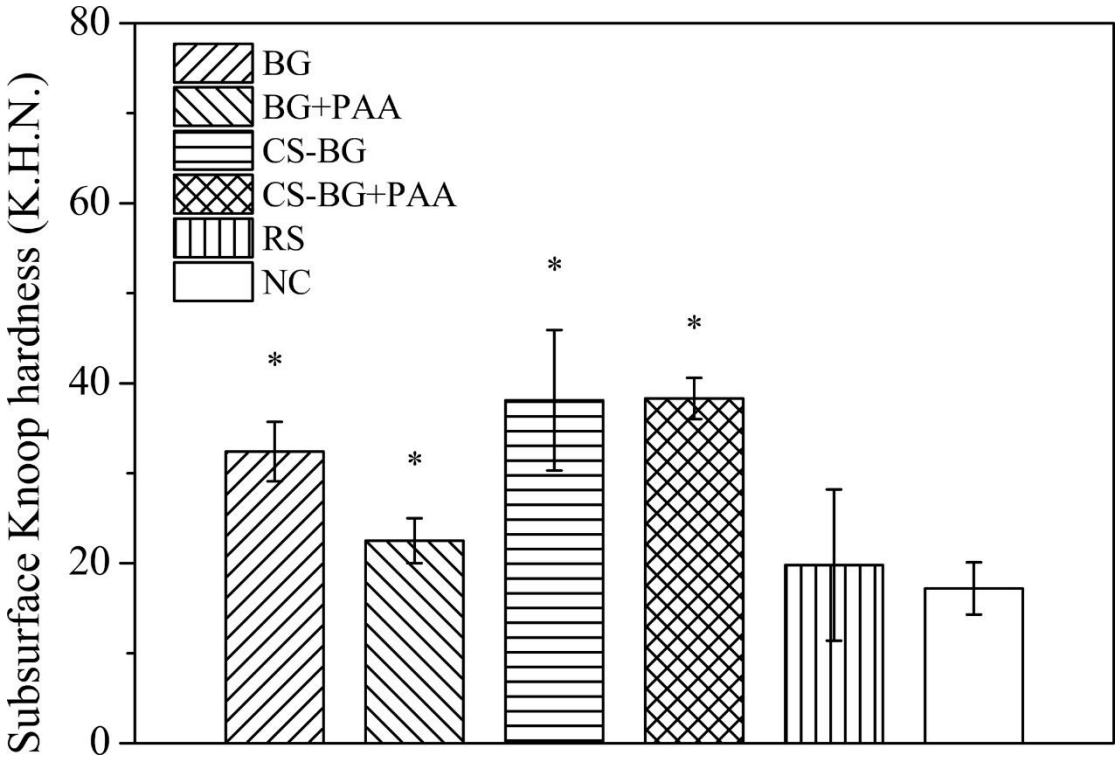

Fig. 5 Knoop microhardness on the subsurface (20 μm below) after pH-cycling (Mean ± S.D., K.H.N). All experimental groups except RS (19.8 ± 8.4) have significantly greater subsurface microhardness compared to NC (17.2 ± 2.9) ($p < 0.05$). CS-BG (38.1 ± 7.8) and CS-BG+PAA (36.6 ± 2.4) exhibit larger average hardness than BG (32.4 ± 3.3) and BG+PAA (22.5 ± 2.5). "*" indicates statistical difference compared to NC.

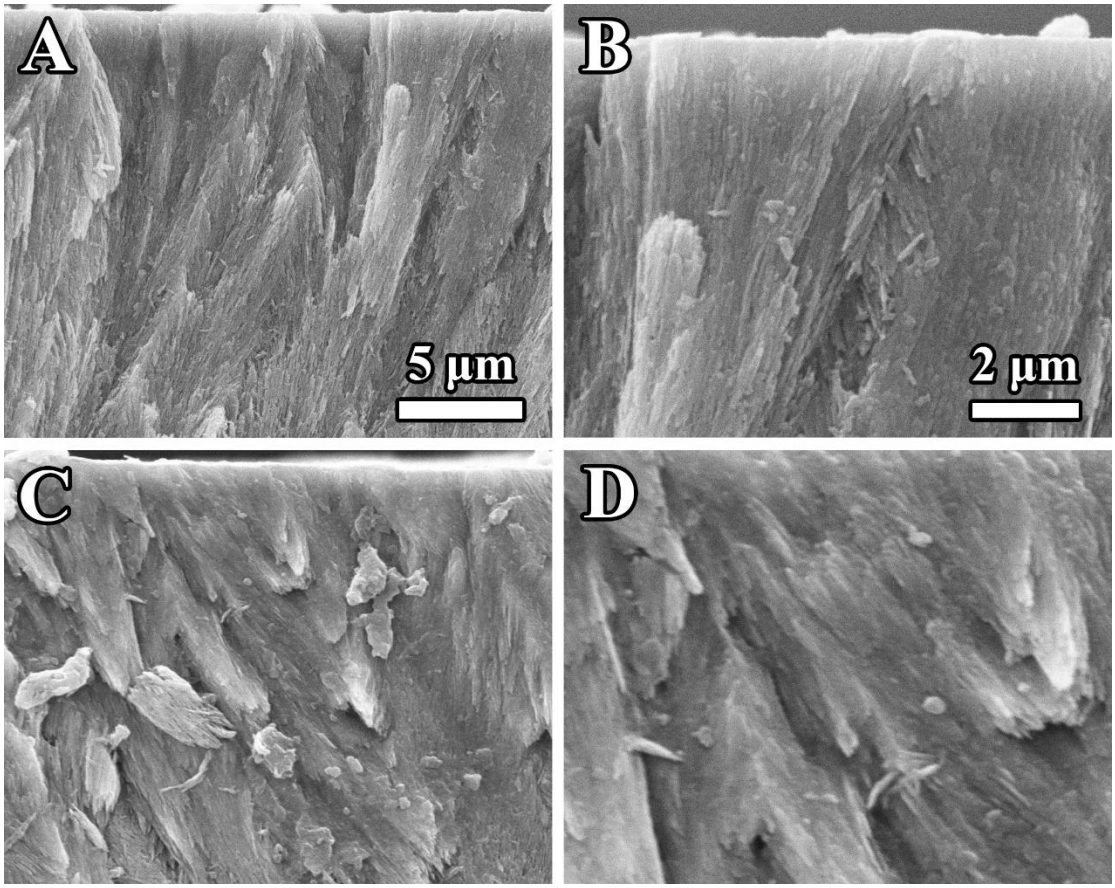

Fig. 6 Representative SEM micrographs of the subsurface of BG (a, b) and CS-BG (c, d) at x4000 and x10000 magnifications. Classical prism structure could be recognised in BG (a) with crystals orientated upwards (b). Whilst in CS-BG, the prism structure is difficult to distinguish with tightly bonded crystals this tight bonded across the entire depth of the cross-section examined (c). At higher magnification, the crystal structure is rougher in BG than that in CS-BG.

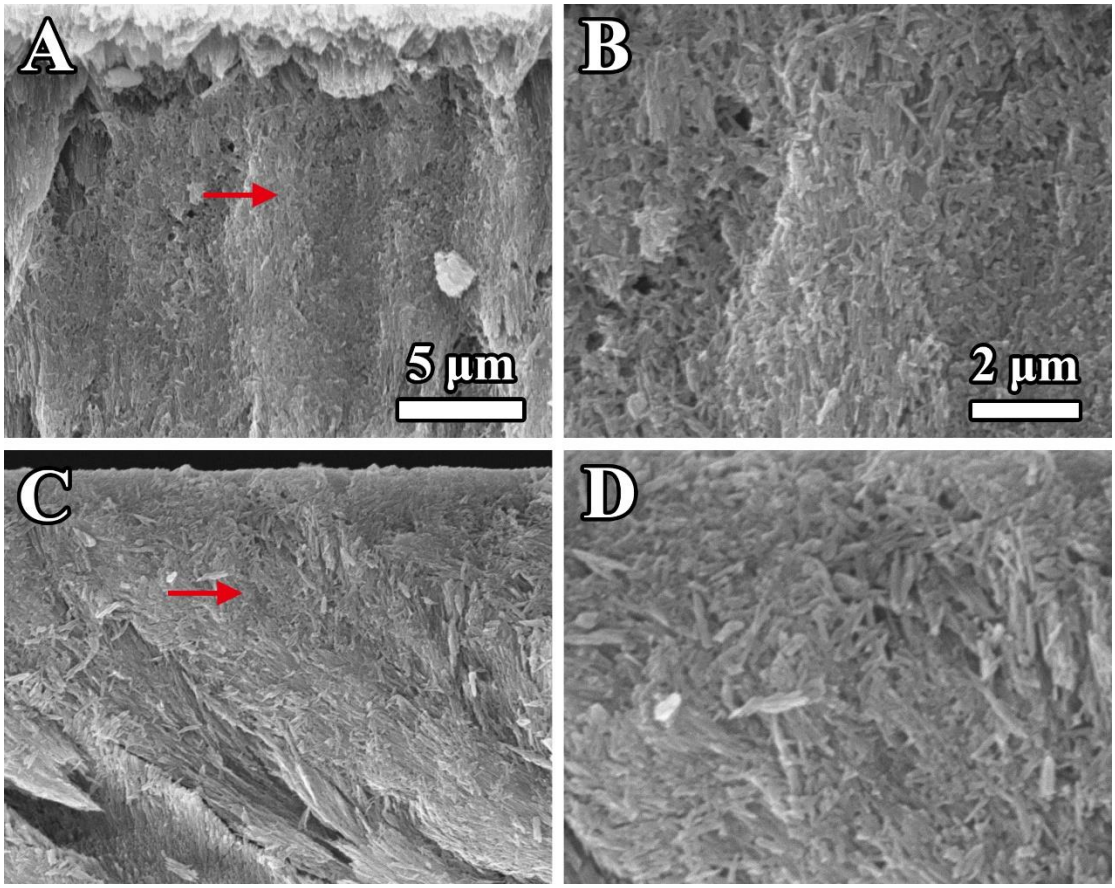

Fig. 7 Representative SEM micrographs of the subsurface of BG+PAA (a, b) and CS-BG+PAA (c, d) at x4000 and x10000 magnifications. A coating composed of newly-deposited crystals were found in both samples (red arrows). At higher magnification, it can be seen that crystals in BG+PAA are smaller and shorter compared to those in CS-BG+PAA which are more enamel-like. Both coating layers are porous and partially cover prisms with some porosities exposed.

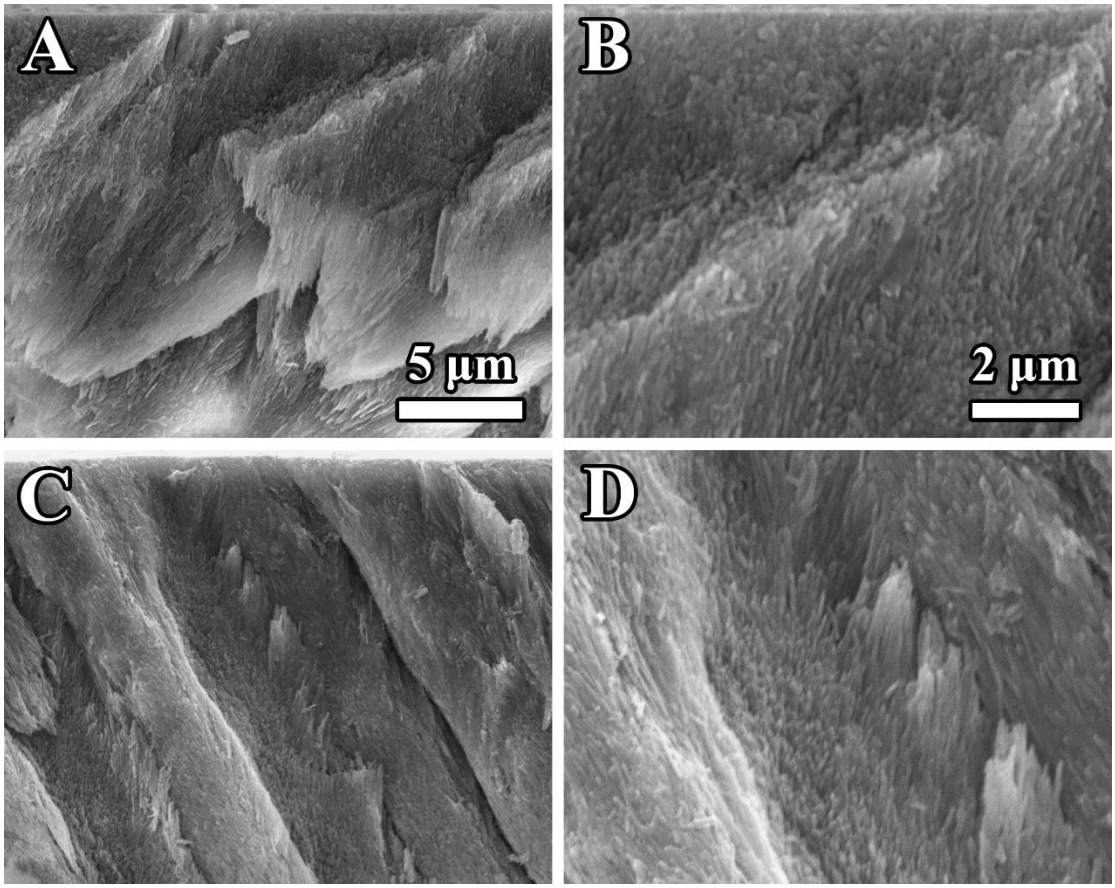

Fig. 8 Representative SEM micrographs of the subsurface of RS (a, b) and NC (c, d) at x4000 and x10000 magnifications. Typical prismatic structure can be recognised in both groups (a, c). Porosities derived from demineralisation are clearly seen at higher magnification and no obvious mineral depositions are found (c, d).